Journal of Mining and Environment (JME) Vol. 13, No. 2, 2022, 559-577

Shahrood University of Technology

Iranian Society of Mining Engineering (IRSME)

Journal of Mining and Environment (JME)

journal homepage: www.jme.shahroodut.ac.ir

THOMSON REUTERS

Effect of Glass and Polypropylene Hybrid Fibers on Mode I, Mode II, and Mixed-Mode Fracture Toughness of Concrete Containing Micro-Silica and Limestone Powder

Danial Fakhri, Mehdi Hosseini*, Mahdi Mahdikhani

Department of mining engineering, Imam Khomeini international university, Ghazvin, Iran

Article Info

Received 20 May 2022

Received in Revised form 26 May 2022

Accepted 29 May 2022

Published online 29 May 2022

DOI:10.22044/jme.2022.11936.2188

Keywords

Fracture toughness

Micro-silica

Limestone powder

Glass and polypropylene hybrid fibers

Mixed mode

Abstract

Fracture toughness is an important concrete property that controls crack extension and concrete fracture. Concrete is the most widely used material in civil engineering containing the most conventional and cheapest materials. Accordingly, cracks and fractures may cause irreparable damages. To this end, fibre-reinforced concretes have been recently constructed in order to overcome the aforementioned weaknesses. Crack propagation and fracture toughness of various concrete specimens are analyzed by the straight notched Brazilian disc (SNBD) test. The specimens are conventional concrete lacking micro-silica and limestone powder, and those containing various volume percentages of fibers including the concrete specimens containing 0.35% individual polypropylene (PP) fibers, 0.35% individual glass fibers, concrete specimens containing 0.17% PP and 0.18% glass fibers, and concrete fibers containing 0.1% PP and 0.25% glass fibers. Micro-silica has replaced 10 wt% cement in all fiber-reinforced concrete specimens, and limestone has replaced 5 wt% cement. Crack extension from the pre-existing cracks in the specimens and mode I, mode II, and mixed-mode fracture toughness are calculated. The BD test is performed on the specimens at the crack inclination angles of 0°, 15°, 28.83°, 45°, 60°, 75°, and 90°. The experimental results show the initiation of wing cracks at angles less than 60° ($0 < \alpha < 60°$) from the tip of the pre-existing cracks. The crack growth and propagation path approach the loading direction by continuing loading. However, the cracks are initiated at a distance of d from the crack tip at angles larger than 60°. The observed distance is larger in the fiber-less specimens than in the fiber-reinforced specimens. The concrete specimens reinforced by 0.17% PP and 0.18% glass hybrid fibers containing micro-silica and limestone powder showed the highest mode I, mode II, and mixed-mode fracture toughness compared to the other concrete specimens.

1. Introduction

In a broad sense, concrete refers to any material or compound consisting of a cementitious adhesive. Concrete is among the key building materials, increasingly consumed in all countries for multiple reasons. Studying crack development, extension, and joining plays a vital role in predicting the fracture process, as rock or concrete is eventually fractured by joining and alternative growth of cracks [1]. Fracture toughness is among the critical mechanical properties that control crack extension and rock fracture. In the fracture mechanics science, the stress intensity factor estimates the critical conditions of a notched piece at the crack tip. The stress intensity factor (K) determines the local stress at the crack tip. Thin fibers uniformly dispersed in the concrete matrix have been used in the recent decades in order to provide the isotropic conditions and reduce the brittleness of concrete. The physical properties of fiber-reinforced concretes are considerably

* *Corresponding author: mahdi_hosseini@eng.ikiu.ac.ir (M. Hosseini).*

influenced by the fiber properties including the volume ratio of fibers, matrix type, fiber orientation, and bonds between fibers [2]. Therefore, it is necessary to investigate the effect of fibers on crack propagation and fracture toughness in designing the concrete structures and reducing the damages caused by this process as much as possible. Accordingly, this study investigates the effect of glass and PP hybrid fibers on mode I, mode II, and mixed-mode fracture toughness of concrete containing micro-silica and limestone powder under various loading angles.

Synthetic fibers are currently used to improve the concrete mechanical properties. In particular, glass, carbon, and steel fibers used in concrete have improved several properties of concrete, inspired by old techniques of using natural fibers [3].

The use of fibers in concrete changes its physical and mechanical properties. Accordingly, numerous studies have been conducted on the effect of fibers on the physical, mechanical, and toughness of concrete. For example, Song and Hwang have used 0.5 vol%, 1.5 vol%, and 2 vol% steel fibers. Their results showed that the compressive strength of concrete reinforced with 0.5 vol%, 1.5 vol%, and 2 vol% fibers increased by 7%, 15.3%, and 12.9%. The tensile strength of concrete containing 0.5-2 vol% increased by 19% to 98.3% [4]. Karahan *et al.* have used 0.05 vol% PP fibers finding 2.4% increase in the compressive strength of fiber-reinforced concrete relative to fiber-less concrete. However, the compressive strength decreased by 1.9% and 3% by increasing fiber percentage to 0.1 vol% and 0.2 vol%, respectively [5]. Choi and Yuan have found that the compressive strength of fiber-reinforced concrete containing 1% and 1.5% PP fibers decreased by 0.4% and 16.5% relative to control concrete. The compressive strength of specimens containing 1% and 1.5% glass fibers decreased by 27.5% and 29.3%, respectively. The tensile strength of concrete reinforced with 1% and 1.5% PP fibers increased by 16% and 16.6% relative to control concrete. Adding 1% and 1.5% glass fibers increased the tensile strength of fiber-reinforced concrete by 11 and 21% relative to control concrete, respectively [6]. According to Prathipati *et al.* the compressive and tensile strength of the specimens containing 1.25% steel fibers and 0.4% glass fibers improved by 14% and 44%, respectively [7]. Taherifard *et al.* have found that adding 0.1 vol%, 0.2 vol%, and 0.3 vol% PP fibers decrease the compressive strength of fiber-reinforced concrete by 2.5%, 4.9%, and 11.5%, respectively. Adding 0.1 vol%, 0.2 vol%, and 0.3 vol% glass fibers decreased the compressive strength by 0.8%, 2.8%, and 6.5%, respectively [8]. Aslani and Nejati have added 0.38 vol% steel fibers and 0.55 vol% PP fibers to concrete. The compressive strength of concrete reinforced by steel and PP fibers increased by 10% and 2.7%, respectively. However, the tensile strength of concrete reinforced by steel fibers increased by 19%, and that reinforced by PP fibers decreased by 3.5% [9]. Patel *et al.* have investigated the effect of recycled glass fibers and found an increase in the compressive and tensile strength of 28- and 7-day specimens. The maximum tensile strength of the specimen containing 0.3% recycled glass fibers was 3.46 MPa (2.48 MPa for fiber-less specimen) [10].

According to Hatami Jorbatet *et al.*, adding 0.2% glass fibers decreased the compressive strength by 1.19%, and increased the tensile strength by 1.3% relative to the control specimen. Adding 0.35 vol% and 0.5 vol% glass fibers increased the compressive strength by 7.2% and 4.7% and decreased the tensile strength by 12.7% and 4.2% relative to fiber-less concrete [11]. There are also studies on fracture toughness. For instance, Ghazvinian *et al.* have studied crack extension in the central straight notched Brazilian disc (CSNBD) specimen made of pozzolanic cement, plaster, and water in the mixed-mode (I-II). The experimental results showed the inverse relationship between the loading angle and K_{IC}. However, K_{IIC} first increased from 0 to 45°, and then decreased as the loading angle increased from 45° to 90° [12]. According to Golewski and Marek Gil, adding micro-silica to concrete significantly increased fracture toughness of the young-age concrete specimens [13].

Abou El-Mall et al. have calculated the mode II fracture toughness (K_{IIC}) of fiber-reinforced concrete for a wide range of materials. According to their results, the mode II fracture toughness (K_{IIC}) of concrete containing glass and steel hybrid fibers was higher than the other patterns [14]. By testing the straight notched Brazilian disc (SNBD) specimens, crack propagation and fracture toughness in fiber-less concrete specimens and those containing 0.2 vol%, 0.35 vol%, and 0.5 vol% glass and PP fibers were studied. The specimens containing 0.2 vol% glass fibers showed the highest fracture toughness. Cracks were initiated at crack inclination angles ≤

60° with the growth of wing cracks from the notch tip. However, cracks were initiated at a distance odd from the pre-existing crack tip at 75° and 90° [15].

According to the literature, there are studies on the fracture toughness of the materials other than concrete or those lacking fibers or containing individual fibers. This experimental study investigates the effect of PP and glass hybrid fibers on mode I, mode II, and mixed-mode fracture toughness of concrete containing micro-silica and limestone powder as the most widely used building materials.

2. Specimens

In order to examine the effect of fiber type, micro-silica, and limestone powder on mode I, mode II, and mixed-mode crack propagation in fiber-reinforced concrete specimens, conventional concrete lacking micro-silica and limestone powder, concrete containing 10% micro-silica and 5% limestone powder with glass fibers, concrete containing 10% micro-silica and 5% limestone powder with PP fibers, concrete containing 10% micro-silica and 5% limestone powder with glass and PP hybrid fibers were prepared for the CSNBD test to determine the mode I, mode II, and mixed-mode fracture toughness. The fracture toughness test was performed at the crack inclination angles of 0°, 15°, 28.83°, 45°, 60°, 75°, and 90°. Twenty-eight specimens were considered for each mode, including 28 Brazilian concrete discs lacking fibers, micro-silica, and limestone, 28 Brazilian concrete discs containing 0.35 vol% glass fibers, 10% micro-silica, and 5% limestone powder, 28 Brazilian concrete discs containing 0.35% PP fibers, 10% micro-silica, and 5% limestone powder, 28 Brazilian concrete discs containing 0.18% glass fibers, 0.17% PP fibers, 10% micro-silica, and 5% limestone powder, and 28 Brazilian concrete discs containing 0.25% glass fibers, 0.1% PP fibers, 10% micro-silica, and 5% limestone powder. The 28-day specimens were tested.

Figures 1 and 2, respectively, show the PP and glass fibers used in this study. Tables 1 and 2 report specifications of the fibers purchased from Iran Boress Co. Table 3 presents the mix designs of conventional concrete and concretes reinforced by PP fibers, glass fibers, and glass and PP hybrid fibers containing micro-silica and limestone powder.

Figure 1. Polypropylene fibers.

Figure 2. Glass fibers.

Table 1. Specifications of polypropylene fibers [16].

Diameter (µm)	18
Density (g/cm3)	0.91
Modulus of elasticity (GPa)	5
Tensile strength (GPa)	0.5
Softening point (°C)	140-150
Melting point (°C)	160-170

Table 2. Specifications of glass fibers [16].

Diameter (µm)	15-30
Density (g/cm3)	2.75
Modulus of elasticity (GPa)	70
Tensile strength (GPa)	3
Softening point (°C)	530-540
Melting point (°C)	550-560

Table 3. Mix designs of concretes.

Components	Conventional concrete lacking fibers, micro-silica and limestone powder (content per per m3 concrete)	PP fiber-reinforced concrete containing micro-silica and limestone powder (content per per m3 concrete)	Glass fiber-reinforced concrete containing micro-silica and limestone powder (content per per m3 concrete)	Glass and PP hybrid fibers-reinforced concrete containing micro-silica and limestone powder (content per per m3 concrete)
Type 2 Portland Cement (kg)	350	297.5	297.5	297.5
Sand (kg)	1150	1150	1150	1150
Gravel (kg)	700	700	700	700
Microsilica (wt% relative to cement)	0	10	10	10
Limestone powder (wt% relative to cement)	0	5	5	5
PP fibers (kg)	0	3.185	0	0.91, 1.54
PP fibers (vol% relative to concrete)	0	0.35	0	0.1, 0.17
Glass fibers (kg)	0	0	9.625	4.95, 6.87
Glass fibers (vol% relative to concrete)	0	0	0.35	0.18, 0.25
Water/cement ratio	0.4	0.4	0.4	0.4
Super-plasticizer (wt% relative to cement)	0.8	0.8	0.8	0.8

The specimens were sent to the XRF laboratory of The Geology and Mineral Exploration Organization. Table 4 presents the XRF results for sand and gravel used to prepare the concrete specimens, according to the screen analysis, sand used in this study meet requirements of National Standard No. 302, Institute of Standards and Industrial Research of Iran [17].

Table 4. XRF results for sand and gravel.

Sample	Unit	Sio_2	Al_2O_3	Fe_2O_3	Na_2O	K_2O	CaO	MgO	SO_3	P_2O_5	MnO	TiO_2	L.O.I
Sand	%	3.3	0.9	0.6	<0.1	0.2	52.8	0.6	< 0.1	< 0.1	< 0.1	< 0.1	41.4
Gravel	%	7.3	1.6	1	0.4	0.5	49.3	0.9	< 0.1	< 0.1	< 0.1	< 0.1	38.8

Special models constructed according to the SNBD design (Fig. 3) were used to prepare te specimens. The width of the mold was 9.5 cm and its length was 38 cm. According to the dimensions mentioned in Table 5, it was possible to prepare 4 discs in one mold.

Table 5. Specifications of notched discs for fracture toughness test.

Mean thickness of specimens (mm)	Mean thickness of specimens (mm)	Mean crack length (mm)
75	25	15

Figure 3. Molds constructed to prepare SNBD concrete specimens.

After preparing the concrete, the mixture was poured in the streel model. Concrete remained in the model for 24 h after leveling its upper surface. The specimens were removed from the molds and stored for 28 days in lime water in the laboratory at 23 ± 2°C according to the Iran National Standard requirements [18].

3. Testing Straight Notched Brazilian Disc (BD) Specimens

This test was developed by Awaji and Sato (1978) in order to measure the mixed-mode fracture toughness of the graphite, plaster, and marble specimens. Atkinson introduced the shear intensity factor for this method, which could be used to determine the mode I, mode II, and mixed-mode fracture toughness [19]. Figure 4 schematically shows the geometry of the BD specimen.

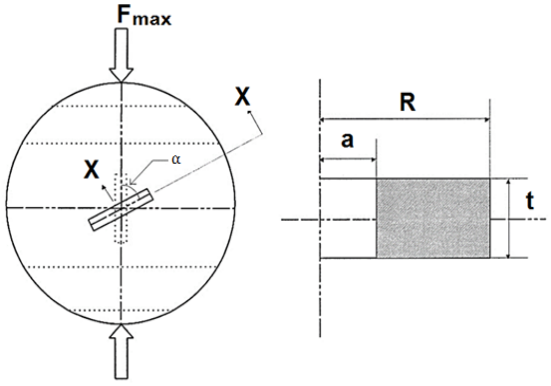

Figure 4. Geometry of BD specimen [11].

The mode I, mode II, and mixed-mode fracture toughness was calculated from Eqs. 1-5 [19]

$$K_{IC} = \frac{F_{max}\sqrt{a}}{\sqrt{\pi}Rt} N_I \quad (1)$$

$$N_I = 1 - 4\,sin^2\alpha + 4\,sin^2\,\alpha\ (1 - 4\,cos^2\alpha)\left(\frac{a}{R}\right)^2 \quad (2)$$

$$K_{IIC} = \frac{Fmax\sqrt{a}}{\sqrt{\pi}Rt} N_I \quad (3)$$

$$N_{II} = \left[2 + (8\,cos^2\,\alpha - 5)\left(\frac{a}{R}\right)^2\right] \sin 2\alpha \quad (4)$$

where K_{IC} and K_{IIC} are the mode I and mode II fracture toughness, Fmax load at failure, R disc radius, t disc thickness, a crack half-length, α crack angle relative to the loading direction, and NI and NII are dimensionless coefficients for mode I and mode II when a/R ≤ 0.3. The angle α equals zero to calculate the pure mode I fracture toughness. Moreover, $N_I = 0$ to calculate the pure mode II angle from Eq. 2 [20].

$$K_{eff} = \sqrt{{K_I}^2 + {K_{II}}^2} \quad (5)$$

where Keff denotes the effective fracture toughness [20]. Figure 5 shows the mixed-mode fracture toughness test on the BD concrete specimen.

Figure 5. Mixed-mode fracture toughness on BD concrete specimen.

Failure mode is mode I (tensile mode) at the 0 and 90 degree inclination angles, mode II (shear mode) at the 28.83 degree inclination angle, and mixed mode at other angles.

4. Test results on concrete specimens containing micro-silica and limestone powder

Tables 6 and 7 report the results of the fracture toughness test.

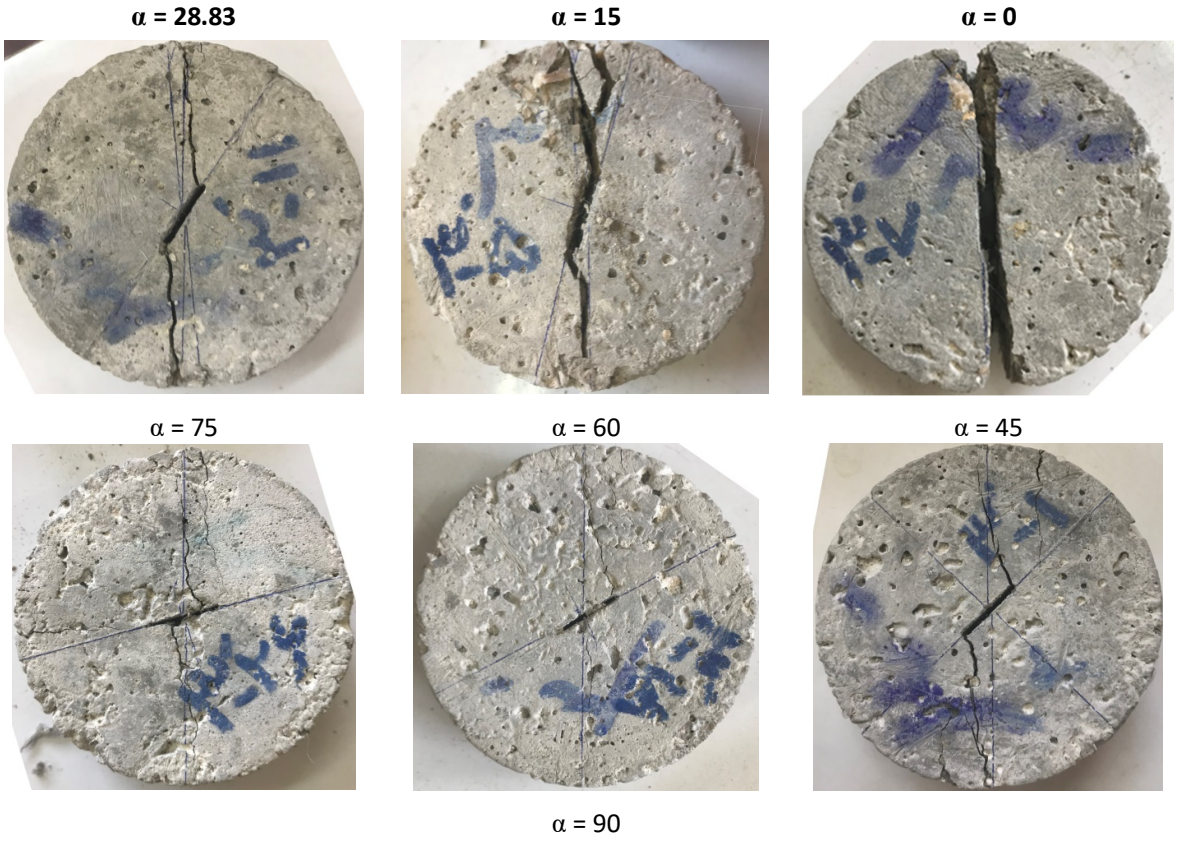

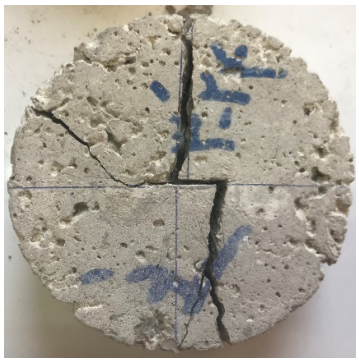

Figure 6: Failure of concrete specimens containing 0.35 glass fibers, micro-silica, and limestone powder.

Table 6. Fracture toughness test results for fiber-less concrete specimen lacking micro-silica and limestone powder and the concrete specimen containing individual PP and glass G fibers and micro-silica and limestone powder.

Specimen code	Loading angle (°)	Fiber content (vol% relative to concrete)	Failure mode	Crack initiation angle (°)	Crack distance from the pre-crack tip (mm)	K_{IC} (MPa.m$^{1/2}$)	K_{IIC} (MPa.m$^{1/2}$)	K_{eff} (MPa.m$^{1/2}$)
1-3	0	-	I	0	0	0.52	0	0.52
1-12	0	-	I	0	0	0.55	0	0.55
1-13	0	-	I	0	0	0.43	0	0.43
1-18	0	-	I	0	0	0.50	0	0.49
1-8	15	-	Mixed	22.15	0	0.32	0.49	0.58
1-9	15	-	Mixed	21.15	0	0.33	0.50	0.60
1-14	15	-	Mixed	23	0	0.29	0.44	0.53
1-19	15	-	Mixed	22.4	0	0.32	0.49	0.58
1-4	28.83	-	II	44.73	0	0	0.71	0.71
1-6	28.83	-	II	51.68	0	0	0.69	0.68
1-20	28.83	-	II	45.37	0	0	0.85	0.85
1-27	28.83	-	II	44.37	0	0	0.68	0.67

Table 6. Continuous of Table 6

Specimen code	Loading angle (°)	Fiber content (vol% relative to concrete)	Failure mode	Crack initiation angle (°)	Crack distance from the pre-crack tip (mm)	K_{IC} (MPa.m$^{1/2}$)	K_{IIC} (MPa.m$^{1/2}$)	K_{eff} (MPa.m$^{1/2}$)
1-2	45	-	Mixed	59.97	0	-0.42	0.75	0.86
1-5	45	-	Mixed	64	0	-0.42	0.74	0.84
1-15	45	-	Mixed	56.93	0	-0.41	0.73	0.83
1-26	45	-	Mixed	60.48	0	-0.44	0.79	0.90
1-1	60	-	Mixed	72.63	4.95	-0.81	0.66	1.04
1-17	60	-	Mixed	75	5.31	-0.83	0.66	1.06
1-21	60	-	Mixed	78.98	5.23	-0.79	0.64	1.02
1-25	60	-	Mixed	86.58	5	-0.82	0.66	1.05
1-7	75	-	Mixed	89.29	6.9	-1.21	0.41	1.27
1-11	75	-	Mixed	92.67	7	-1.15	0.40	1.21
1-24	75	-	Mixed	86.58	6.41	-1.16	0.40	1.22
1-10	90	-	I	95	7.5	-1.34	0	1.33
1-16	90	-	I	90.35	7.6	-1.30	0	1.29
1-22	90	-	I	90.44	7.4	-1.39	0	1.39
1-23	90	-	I	106.3	7.3	-1.36	0	1.36
PP-18	0	0.35 PP	I	0	0	0.47	0	0.47
PP-20	0	0.35 PP	I	0	0	0.42	0	0.42
PP-27	0	0.35 PP	I	0	0	0.53	0	0.53
PP-30	0	0.35 PP	I	0	0	0.37	0	0.37
PP-9	15	0.35 PP	Mixed	29	0	0.31	0.46	0.55
PP-11	15	0.35 PP	Mixed	28	0	0.34	0.51	0.62
PP-16	15	0.35 PP	Mixed	28	0	0.39	0.58	0.70
PP-17	15	0.35 PP	Mixed	26	0	0.33	0.50	0.59
PP-21	28.83	0.35 PP	II	43.15	0	0	0.72	0.72
PP-23	28.83	0.35 PP	II	45	0	0	0.73	0.73
PP-26	28.83	0.35 PP	II	46.33	0	0	0.71	0.71
PP-31	28.83	0.35 PP	II	44	0	0	0.77	0.77

PP-4	45	0.35 PP	Mixed	57.44	0	-0.54	0.96	1.10
PP-6	45	0.35 PP	Mixed	56.8	0	-0.46	0.81	0.93
PP-12	45	0.35 PP	Mixed	59.81	0	-0.45	0.81	0.92
PP-28	45	0.35 PP	Mixed	59.14	0	-0.45	0.81	0.93
PP-3	60	0.35 PP	Mixed	76.96	2	-0.89	0.72	1.14
PP-10	60	0.35 PP	Mixed	72	1.77	-0.79	0.65	1.02
PP-22	60	0.35 PP	Mixed	74.44	1.9	-0.99	0.80	1.27
PP-25	60	0.35 PP	Mixed	77	2	-0.98	0.79	1.26
PP-5	75	0.35 PP	Mixed	86	3.5	-1.17	0.40	1.24
PP-8	75	0.35 PP	Mixed	85	3.761	-1.12	0.39	1.18
PP-19	75	0.35 PP	Mixed	85.77	4.8	-1.22	0.42	1.29
PP-29	75	0.35 PP	Mixed	90	3.16	-1.16	0.40	1.23
PP-2	90	0.35 PP	I	94.2	5.15	-1.28	0	1.28
PP-7	90	0.35 PP	I	91	5.2	-1.25	0	1.25
PP-13	90	0.35 PP	I	92	5.5	-1.25	0	1.25
PP-24	90	0.35 PP	I	91	5	-1.32	0	1.32
PP-14	90	0.35 PP	I	91.33	5.33	-1.25	0	1.25
G-4	0	0.35 G	I	0	0	0.49	0	0.49
G-7	0	0.35 G	I	0	0	0.35	0	0.35
G-13	0	0.35 G	I	0	0	0.36	0	0.36
G-15	0	0.35 G	I	0	0	0.55	0	0.55
G-21	0	0.35 G	I	0	0	0.42	0	0.42
G-29	0	0.35 G	I	0	0	0.32	0	0.32
G-16	15	0.35 G	Mixed	33	0	0.33	0.50	0.60
G-23	15	0.35 G	Mixed	34	0	0.33	0.50	0.61
G-25	15	0.35 G	Mixed	36	0	0.39	0.59	0.71
G-31	15	0.35 G	Mixed	35	0	0.35	0.52	0.63
G-5	15	0.35 G	Mixed	31	0	0.39	0.59	0.71
G-9	28.83	0.35 G	II	48	0	0	0.81	0.81
G-11	28.83	0.35 G	II	49	0	0	0.86	0.86
G-24	28.83	0.35 G	II	46.8	0	0	0.81	0.81
G-1	45	0.35 G	Mixed	67	0	-0.42	0.75	0.86
G-12	45	0.35 G	Mixed	70.23	0	-0.49	0.87	1

Table 6. Continuous of Table 6

Specimen code	Loading angle (°)	Fiber content (vol% relative to concrete)	Failure mode	Crack initiation angle (°)	Crack distance from the pre-crack tip (mm)	K_{IC} (MPa.m$^{1/2}$)	K_{IIC} (MPa.m$^{1/2}$)	K_{eff} (MPa.m$^{1/2}$)
G-20	45	0.35 G	Mixed	70	0	-0.48	0.87	0.99
G-27	45	0.35 G	Mixed	70.61	0	-0.45	0.81	0.93
G-8	60	0.35 G	Mixed	84	1.2	-0.93	0.76	1.20
G-18	60	0.35 G	Mixed	82	1.2	-0.87	0.70	1.12
G-30	60	0.35 G	Mixed	76	1.3	-0.89	0.72	1.15
G-32	60	0.35 G	Mixed	79	1.2	-0.86	0.68	1.10
G-3	75	0.35 G	Mixed	87	3.141	-1.29	0.44	1.36
G-17	75	0.35 G	Mixed	89	2.8	-1.24	0.43	1.31
G-26	75	0.35 G	Mixed	87	2.6	-1.20	0.42	1.27
G-28	75	0.35 G	Mixed	88.37	2.65	-1.22	0.42	1.29
G-6	90	0.35 G	I	90	6	-1.34	0	1.34
G-10	90	0.35 G	I	91	6	-1.47	0	1.47
G-19	90	0.35 G	I	91	6	-1.44	0	1.44
G-22	90	0.35 G	I	90.5	6	-1.34	0	1.34

Table 7. Fracture toughness test results for concrete specimen containing PP and G hybrid fibers and micro-silica, and limestone powder.

Specimen code	Loading angle (°)	Fiber content (vol% relative to concrete)	Failure mode	Crack initiation angle (°)	Crack distance from the pre-crack tip (mm)	K_{IC} (MPa.m$^{1/2}$)	K_{IIC} (MPa.m$^{1/2}$)	K_{eff} (MPa.m$^{1/2}$)
PP-G-9	0	0.17 PP، 0.18 G	I	0	0	0.51	0	0.51
PP-G-20	0	0.17 PP، 0.18 G	I	0	0	0.48	0	0.48
PP-G-32	0	0.17 PP، 0.18 G	I	0	0	0.49	0	0.49
PP-G-8	15	0.17 PP، 0.18 G	Mixed	21.18	0	0.36	0.54	0.65
PP-G-11	15	0.17 PP، 0.18 G	Mixed	23	0	0.37	0.56	0.67

PP-G-12	15	0.17 PP، 0.18 G	Mixed	24.35	0	0.38	0.57	0.69
PP-G-21	15	0.17 PP، 0.18 G	Mixed	22.10	0	0.34	0.51	0.61
PP-G-5	28.83	0.17 PP، 0.18 G	II	40.13	0	0	0.73	0.73
PP-G-17	28.83	0.17 PP، 0.18 G	II	37.61	0	0	0.79	0.79
PP-G-18	28.83	0.17 PP، 0.18 G	II	44.65	0	0	0.92	0.92
PP-G-23	28.83	0.17 PP، 0.18 G	II	43.53	0	0	0.79	0.79
PP-G-27	28.83	0.17 PP، 0.18 G	II	42	0	0	0.85	0.85
PP-G-6	45	0.17 PP، 0.18 G	Mixed	60.20	0	-0.50	0.89	1.02
PP-G-10	45	0.17 PP، 0.18 G	Mixed	65.51	0	-0.57	1.02	1.17
PP-G-25	45	0.17 PP، 0.18 G	Mixed	75.55	0	-0.57	1.03	1.18
PP-G-31	45	0.17 PP، 0.18 G	Mixed	60.77	0	-0.49	0.89	1.02
PP-G-14	60	0.17 PP، 0.18 G	Mixed	70	0.90	-0.81	0.65	1.03
PP-G-15	60	0.17 PP، 0.18 G	Mixed	72.35	0.80	-0.82	0.67	1.06
PP-G-16	60	0.17 PP، 0.18 G	Mixed	72.91	1	-1.03	0.83	1.32
PP-G-24	60	0.17 PP، 0.18 G	Mixed	73.50	0.70	-0.83	0.67	1.07
PP-G-3	75	0.17 PP، 0.18 G	Mixed	84.46	3	-1.26	0.43	1.33
PP-G-13	75	0.17 PP، 0.18 G	Mixed	85.47	3	-1.22	0.42	1.30
PP-G-28	75	0.17 PP، 0.18 G	Mixed	87.84	2.70	-1.29	0.45	1.37
PP-G-29	75	0.17 PP، 0.18 G	Mixed	84.46	2.60	-1.22	0.42	1.29
PP-G-30	75	0.17 PP، 0.18 G	Mixed	85	4.40	-1.03	0.35	1.09
PP-G-1	90	0.17 PP، 0.18 G	I	93	5.14	-1.39	0	1.39
PP-G-2	90	0.17 PP، 0.18 G	I	92.23	5.23	-1.44	0	1.44
PP-G-4	90	0.17 PP، 0.18 G	I	92	5.60	-1.21	0	1.21
PP-G-7	90	0.17 PP، 0.18 G	I	94.14	5.90	-1.58	0	1.58
PP-G-19	90	0.17 PP، 0.18 G	I	92.63	4	-1.44	0	1.44
PP-G2-3	0	0.10 PP، 0.25 G	I	0	0	0.43	0	0.43
PP-G2-16	0	0.10 PP، 0.25 G	I	0	0	0.40	0	0.40
PP-G2-31	0	0.10 PP، 0.25 G	I	0	0	0.54	0	0.54
PP-G2-4	15	0.10 PP، 0.25 G	Mixed	27	0	0.30	0.46	0.55
PP-G2-5	15	0.10 PP، 0.25 G	Mixed	26.27	0	0.30	0.45	0.54
PP-G2-7	15	0.10 PP، 0.25 G	Mixed	28.23	0	0.32	0.49	0.58
PP-G2-14	15	0.10 PP، 0.25 G	Mixed	27	0	0.31	0.46	0.56
PP-G2-1	28.83	0.10 PP، 0.25 G	II	40	0	0	0.76	0.76
PP-G2-9	28.83	0.10 PP، 0.25 G	II	40	0	0	0.75	0.75
PP-G2-10	28.83	0.10 PP، 0.25 G	II	40	0	0	0.76	0.76

Table 7. Continuous of Table 7

Specimen code	Loading angle (°)	Fiber content (vol% relative to concrete)	Failure mode	Crack initiation angle (°)	Crack distance from the pre-crack tip (mm)	K_{IC} (MPa.m$^{1/2}$)	K_{IIC} (MPa.m$^{1/2}$)	K_{eff} (MPa.m$^{1/2}$)
PP-G2-13	28.83	0.10 PP، 0.25 G	II	40	0	0	0.75	0.75
PP-G2-22	28.83	0.10 PP، 0.25 G	II	41	0	0	0.86	0.86
PP-G2-2	45	0.10 PP، 0.25 G	Mixed	65	0	-0.47	0.84	0.96
PP-G2-8	45	0.10 PP، 0.25 G	Mixed	62	0	-0.44	0.80	0.92
PP-G2-15	45	0.10 PP، 0.25 G	Mixed	64	0	-0.45	0.80	0.92
PP-G2-24	60	0.10 PP، 0.25 G	Mixed	60	0	-0.46	0.82	0.94
PP-G2-28	60	0.10 PP، 0.25 G	Mixed	61	0	-0.54	0.96	1.10
PP-G2-18	60	0.10 PP، 0.25 G	Mixed	78	2	-0.93	0.76	1.20
PP-G2-20	60	0.10 PP، 0.25 G	Mixed	78	1.32	-0.93	0.75	1.20
PP-G2-21	75	0.10 PP، 0.25 G	Mixed	75	1.90	-0.90	0.72	1.15
PP-G2-25	75	0.10 PP، 0.25 G	mixed	75	1.70	-0.93	0.75	1.20
PP-G2-17	75	0.10 PP، 0.25 G	Mixed	84	4.80	-1.13	0.39	1.20
PP-G2-19	75	0.10 PP، 0.25 G	Mixed	80	4.94	-1.11	0.38	1.17
PP-G2-26	75	0.10 PP، 0.25 G	Mixed	90	4.60	-1.16	0.40	1.23
PP-G2-32	90	0.10 PP، 0.25 G	I	83	4.50	-1.18	0.41	1.24
PP-G2-11	90	0.10 PP، 0.25 G	I	92	5.50	-1.21	0	1.21
PP-G2-12	90	0.10 PP، 0.25 G	I	90	5.50	-1.27	0	1.27
PP-G2-29	90	0.10 PP، 0.25 G	I	90	5.50	-1.20	0	1.20
PP-G2-30	90	0.10 PP، 0.25 G	I	91	5.50	-1.22	0	1.22

Diagrams were plotted to evaluate the crack propagation in different modes, the movie recorded was analyzed with the help of some software, and the results were presented. Figures 7, 8, and 9 show the K_{IC}-α, K_{IIC}-α, and K_{eff} -α diagrams for conventional concrete, concrete containing 0.35% PP, and 0.35% glass fibers. Figures 10 and 11 show the diagrams for hybrid

fiber-reinforced concrete containing 0.17% PP and 0.18% G fibers, and the specimen containing 0.1% PP and 0.25% G hybrid fibers. Figures 12, 13, and 14 show the bar diagrams of different modes for fiber-reinforced concrete specimens containing different glass and PP fiber contents compared to the fiber-less conventional concrete specimen.

Table 8 reports the mean fracture toughness at different crack inclination angles relative to the loading direction.

Table 8. Mean fracture toughness of conventional concrete specimens lacking micro-silica and limestone powder and those containing individual PP fibers, individual G fibres, and PP and G hybrid fibers, micro-silica and limestone powder

Type of concrete	0.35PP			0.35G			0.17PP-0.18G			0.10PP-0.25G			Conventional concrete		
Angle (˚)	K_{IC} (MPa.m$^{1/2}$)	K_{IIC} (MPa.m$^{1/2}$)	K_{eff} (MPa.m$^{1/2}$)	K_{IC} (MPa.m$^{1/2}$)	K_{IIC} (MPa.m$^{1/2}$)	K_{eff} (MPa.m$^{1/2}$)	K_{IC} (MPa.m$^{1/2}$)	K_{IIC} (MPa.m$^{1/2}$)	K_{eff} (MPa.m$^{1/2}$)	K_{IC} (MPa.m$^{1/2}$)	K_{IIC} (MPa.m$^{1/2}$)	K_{eff} (MPa.m$^{1/2}$)	K_{IC} (MPa.m$^{1/2}$)	K_{IIC} (MPa.m$^{1/2}$)	K_{eff} (MPa.m$^{1/2}$)
0	0.44	0.00	0.44	0.49	0.00	0.49	0.50	0.00	0.50	0.42	0.00	0.42	0.47	0.00	0.47
15	0.33	0.49	0.59	0.36	0.54	0.65	0.37	0.55	0.66	0.30	0.46	0.55	0.33	0.50	0.60
28.83	0.00	0.72	0.72	0.00	0.83	0.83	0.00	0.88	0.88	0.00	0.78	0.78	0.00	0.68	0.68
45	0.45	0.81	0.93	-0.49	0.87	1.00	0.55	0.98	1.09	0.46	0.82	0.93	0.41	0.74	0.85
60	0.93	0.75	1.20	-0.93	0.76	1.20	0.93	0.75	1.20	0.93	0.76	1.20	0.81	0.66	1.05
75	1.14	0.40	1.24	-1.24	0.43	1.31	1.26	0.43	1.33	1.15	0.39	1.21	1.15	0.40	1.22
90	1.26	0.00	1.26	-1.40	0.00	1.40	1.46	0.00	1.46	1.23	0.00	1.23	1.35	0.00	1.35

As shown in Figs 8 and 9, the mode I fracture toughness of concrete containing 0.35% PP fibers and micro-silica and limestone powder decreased by 6.38% and 6.6% at 0˚ and 90˚ relative to the fiber-less concrete specimen lacking micro-silica and limestone powder. The mode I fracture toughness of concrete containing 0.35% G fibers and micro-silica and limestone powder decreased by 4.25% and 3.7% at 0˚ and 90˚ relative to the fiber-less concrete specimen lacking micro-silica and limestone powder. The pure shear mode fracture toughness occurring at 28.83˚ increased by 5.88% and 22.05% for the concrete specimen containing 0.35% PP fibers and micro-silica and limestone powder and that containing 0.35% G fibers and micro-silica and limestone powder relative to the fiber-less concrete specimen lacking micro-silica and limestone powder. The effective fracture toughness of concrete reinforced by PP fibers containing micro-silica and limestone powder is larger than that of fiber-less concrete at loading angles between 28.83 ˚ and 75˚. The effective fracture toughness of concrete reinforced by 0.35% G fibers containing micro-silica and limestone powder was larger than the conventional concrete at all angles.

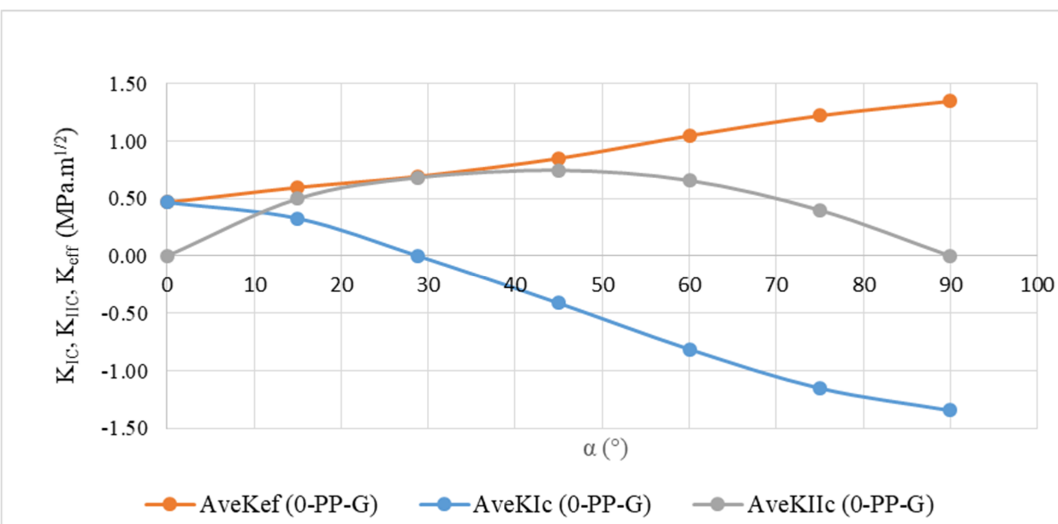

Figure 7. K_{IC}-α, K_{IIC}-α, and K_{eff}-α diagrams for fiber-less concrete lacking micro-silica and limestone powder.

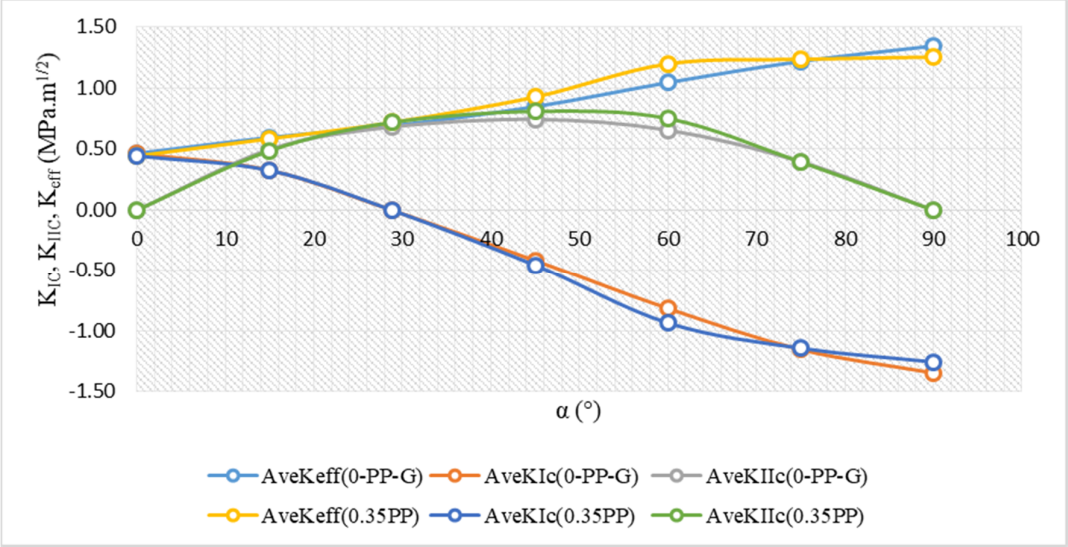

Figure 8. K_{IC}-α, K_{IIC}-α, and K_{eff}-α diagrams for fiber-less concrete lacking micro-silica and limestone powder and concrete reinforced by 0.35% PP fibers containing micro-silica and limestone powder.

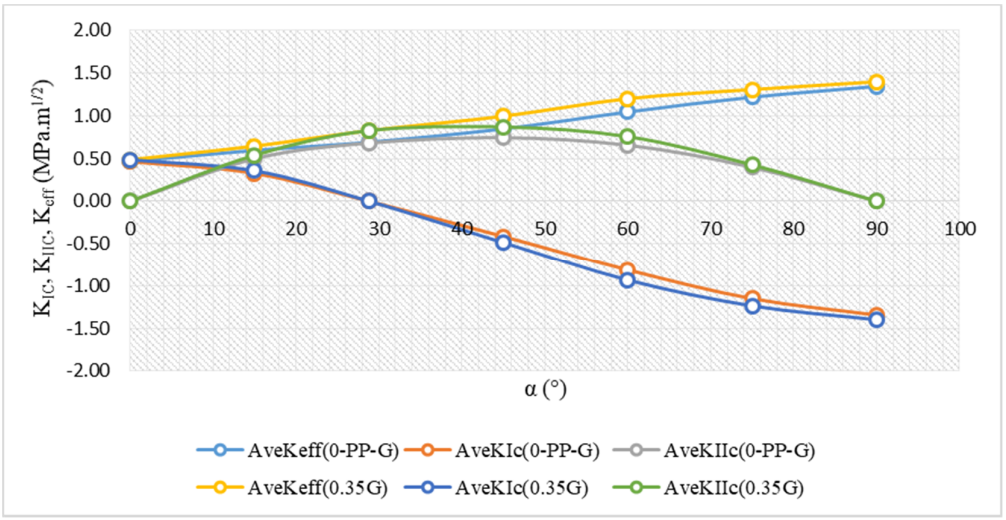

Figure 9. K_{IC}-α, K_{IIC}-α, and K_{eff}-α diagrams for fiber-less concrete lacking micro-silica and limestone powder and concrete reinforced by 0.35% G fibres containing micro-silica and limestone powder.

As shown in Figs 10 and 11, the mode I fracture toughness of concrete reinforced by 0.17% PP and 0.18% G hybrid fibers containing micro-silica and limestone powder and that reinforced by 0.1% PP and 0.25% G hybrid fibers containing micro-silica, and limestone powder decreased by 6.38% and 10.63% at 0° and by 8.14 and 8.88 at 90° relative to the fiber-less concrete specimen. The pure shear mode fracture toughness occurring at 28.83° increased by 27.53% and 14.07% for concrete reinforced by 0.17% PP and 0.18% G hybrid fibers containing micro-silica and limestone powder and that reinforced by 0.1% PP and 0.25% G hybrid fibers containing micro-silica and limestone powder. The effective fracture toughness of concrete reinforced by 0.17% PP and 0.18% G hybrid fibers containing micro-silica and limestone powder increased by 6.38%, 10%, 27.53%, 22.47%, 14.28%, 9.01%, and 8.14% at the inclination angles of 0°, 15°, 28.83°, 45°, 60°, 75°, and 90° relative to the fiber-less concrete specimen. The effective fracture toughness of concrete reinforced by 0.1% PP and 0.25% G hybrid fibers containing micro-silica and limestone powder only increased at inclination angles of 28.83°, 45°, and 60°.

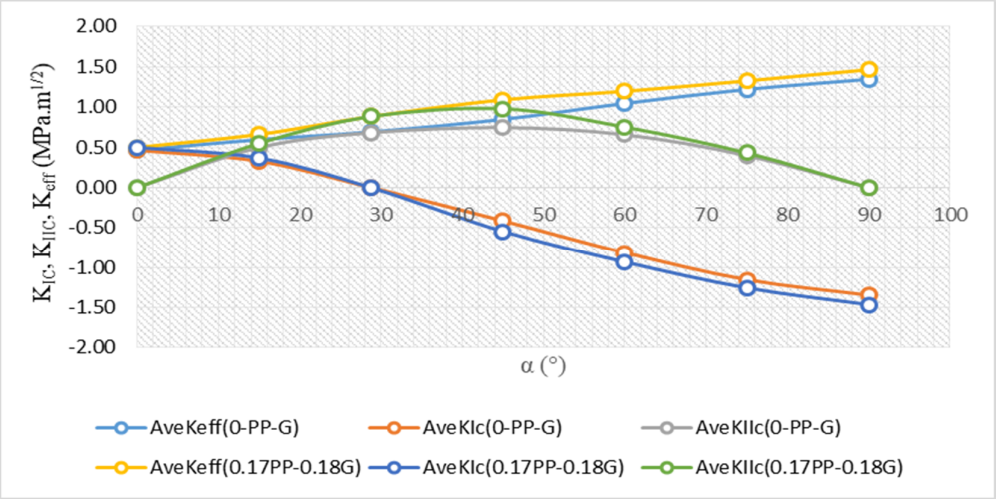

Figure 10. K_{IC}-α, K_{IIC}-α, and K_{eff}-α diagrams for concrete containing micro-silica and limestone powder reinfroced by 0.17% PP and 0.18% G hybrid fibers and the concrete specimen lacking fibers, micro-silica and limestone powder.

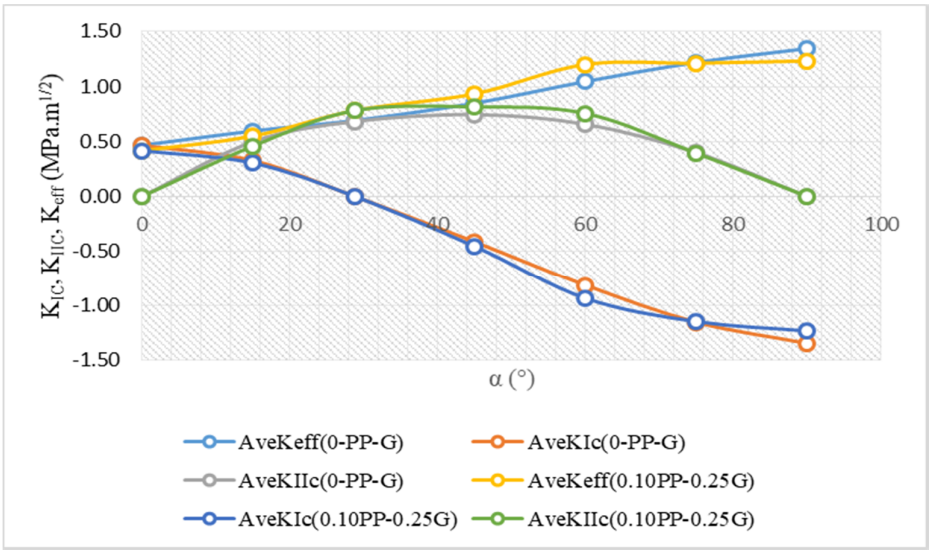

Figure 11. K_{IC}-α, K_{IIC}-α, and K_{eff}-α diagrams for concrete containing micros-ilica and limestone powder reinfroced by 0.1% PP and 0.25% G hybrid fibers and the concrete specimen lacking fibers, micro-silica and limestone powder.

As shown in the bar diagram (Fig. 12), adding 0.35 vol% glass fibers to the concrete and 0.17% PP and 0.18% G hybrid fibers to the concrete containing micro-silica and limestone powder increased the fracture toughness at the inclination angles of 0°, 15°, 28.83°, 45°, 60°, 75°, and 90° relative to the fiber-less concrete lacking micro-silica and limestone powder. The fibers had the highest impact on the fracture toughness of concrete specimens lacking micro-silica and limestone powder and those containing 0.17% PP and 0.18% G hybrid fibers.

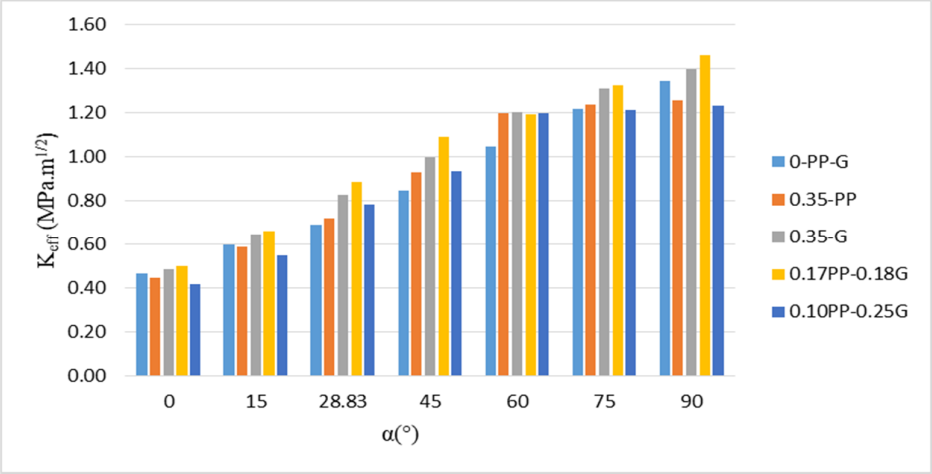

Figure 12. K_{eff}-α bar diagram for concrete lacking fibers, micro-silica, and limestone powder and concrete reinforced by various PP and glass fiber contrents containing micro-silica and limestone powder.

As shown in the bar diagram (Fig. 13), the concrete specimens containing micro-silica and limestone powder reinforced by 0.17% PP and 0.18% G hybrid fibers showed the highest increase in the mode I fracture toughness. The mode I fracture toughness of concrete containing 0.35% glass fibers increased relative to the specimens lacking fibers, micro-silica, and limestone powder at all angles.

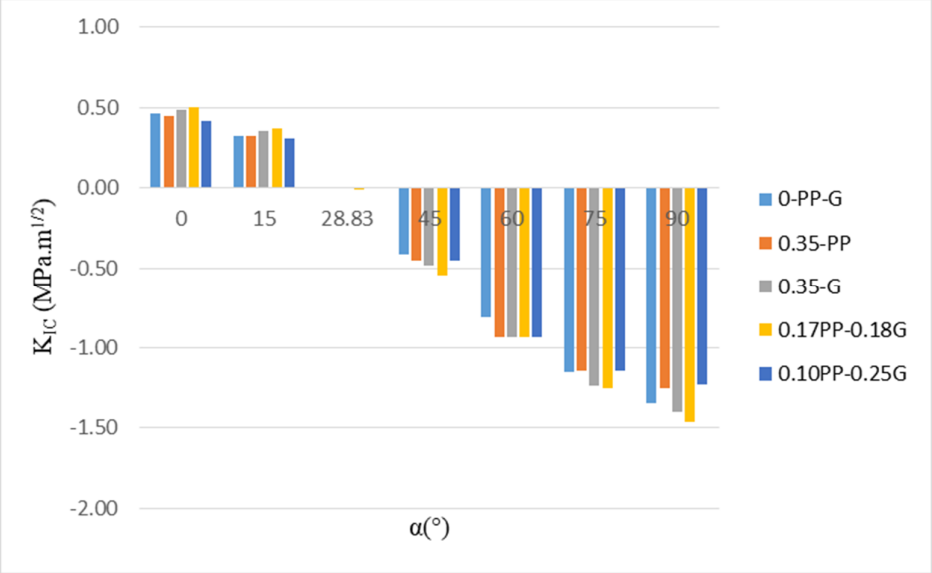

Figure 13. K_{IC}-α bar diagram for concrete lacking fibers, micro-silica, and limestone powder and concrete reinforced by various PP and glass fibre contrents containing micro-silica and limestone powder.

As shown in the bar diagram below (Fig. 14), the concrete specimens containing micro-silica and limestone powder reinforced by 0.17% PP and 0.18% G hybrid fibers showed the highest increase in model II fracture toughness. The pure shear mode fracture toughness occurring at 28.83° increased in all modes. The concrete specimen containing 0.17% PP and 0.18% G hybrid fibers showed the highest increase of 27.53% in the pure shear mode fracture toughness relative to concrete lacking fibers, micro-silica, and limestone powder.

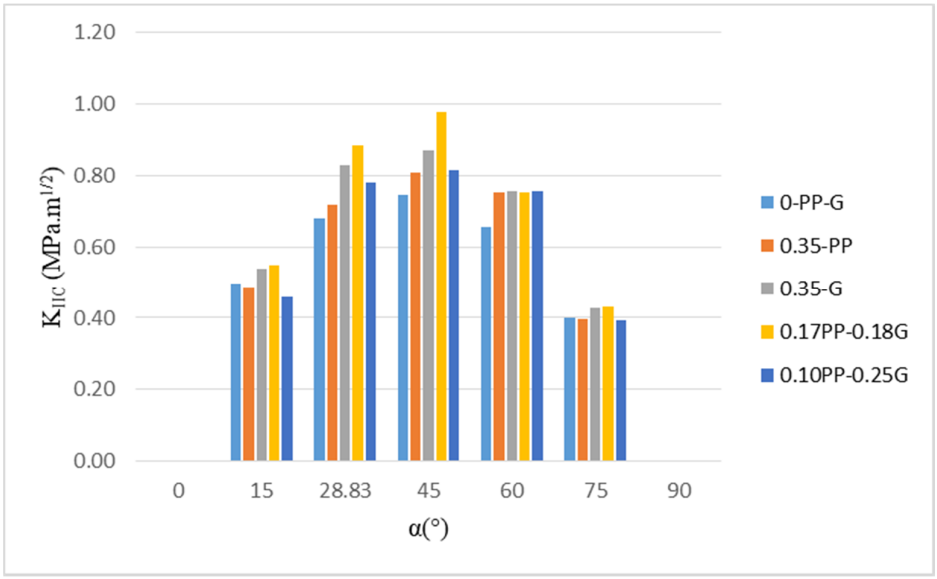

Figure 14. K_{IIC}-α bar diagram for concrete lacking fibers, micro-silica, and limestone powder and concrete reinforced by various PP and glass fiber contents containing micro-silica and limestone powder.

As shown in Fig. 15, the load at failure of the concrete specimens containing micro-silica and limestone reinforced by 0.17% PP and 0.18 G hybrid fibers is larger than specimens lacking fibers, micro-silica, and limestone powder at all inclination angles.

According to the load-failure curves, the slope of the diagram increases up to the inclination angle of 15° for the specimens containing 0.35% glass fibers and concrete containing 0.18% G and 0.17% PP hybrid fibers. The slope is turned negative with increasing the pre-crack inclination angle from 15° to 60° and then positive as the angle increases from 60° to 90°. This uptrend is also observed up to 15° and 28.83°, respectively, for the concrete specimen reinforced by 0.35% PP fibers and the specimen reinforced by 0.1% PP and 0.25% G hybrid fibers. The lowest load at failure is observed at inclination angle of 45° for fiber-less concrete, the specimen containing 0.35% PP fibers, and that reinforced by 0.1% PP and 0.25% G hybrid fibers. The lowest load of rock failure is observed at the inclination angle of 60° for glass fiber-reinforced concrete and the specimen reinforced by 0.17% PP and 0.18% G hybrid fibers. Mirzaei Nasirabad *et al.* have tested the notched Brazilian plaster discs. According to their results, among the notched disc specimens, the disc with an angle of 45° showed the lowest load at failure [21]. The use of concrete containing micro-silica, limestone powder and 0.17% G and 0.18% PP hybrid fibers improved the load at failure by 31.92% and 17.33%, respectively, at 45° and 60° relative to the concrete lacking fibers, micro-silica, and limestone powder. The concrete discs containing 0.18% glass fibers, 0.17% PP fibers, 10% micro-silica, and 5% limestone powder had the maximum load at failure because compared to other concrete discs, these concrete discs had the highest dry unit weight, the highest longitudinal wave velocity, and the lowest effective porosity.

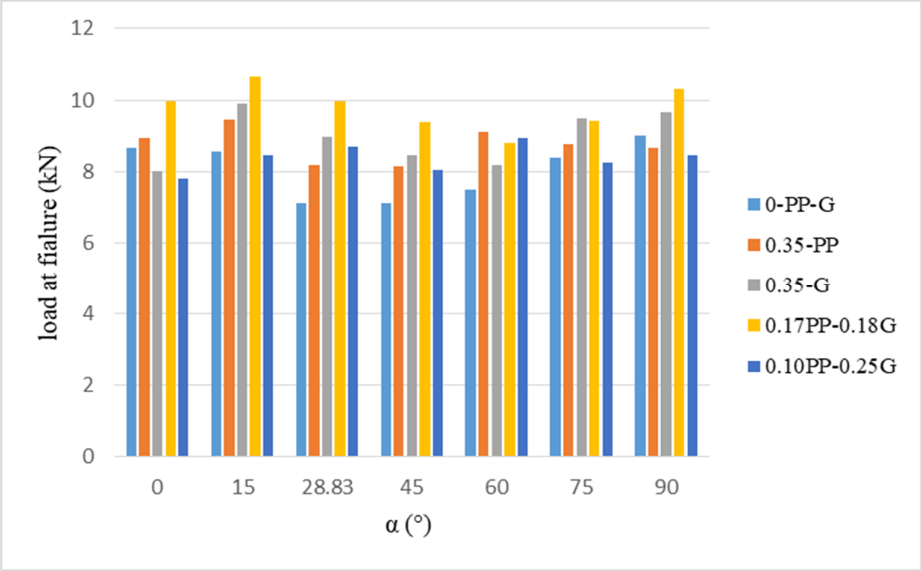

Figure 15. Relationship between load at failure and crack inclination angle for concrete lacking fibers, micro-silica, and limestone powder and concrete containing different percentages of fibers, micro-silica and limestone powder.

Figure 16 shows the changes in the crack initiation angle versus the pre-crack angle. As shown, the crack initiation angle increases with increasing the crack angle relative to the loading direction. Crack extension at $\alpha \leq 45^{\circ}$ is initiated from the pre-crack tip. However, at $\alpha \geq 60^{\circ}$, wing cracks are initiated at a distance of d from the pre-crack tip, and extended to the loading location. With increasing the loading angle up to 75°, the crack extension angle reaches 86°, and this angle reaches 90° when the crack inclination angle approaches 90°. This observation is consistent with the Mirzaei Nasirabad *et al.* studies [21]. They found that the crack propagation angle was vertical when the crack was horizontal, causing two tensile cracks from the center of the notched Brazilian disc specimen. Crack propagation occurs at the maximum compressive load, and wing cracks reach the upper and lower boundaries of the specimen. All other specimens show a lower crack extension angle at the inclination angles of 75° and 90° than the concrete lacking fibers, micro-silica, and limestone powder. The crack initiation angle of the specimens containing 0.35% glass fibers is larger than that of specimens lacking fibers, micro-silica, and limestone powder at the inclination angles of 15°, 28.83°, 45°, and 60°.

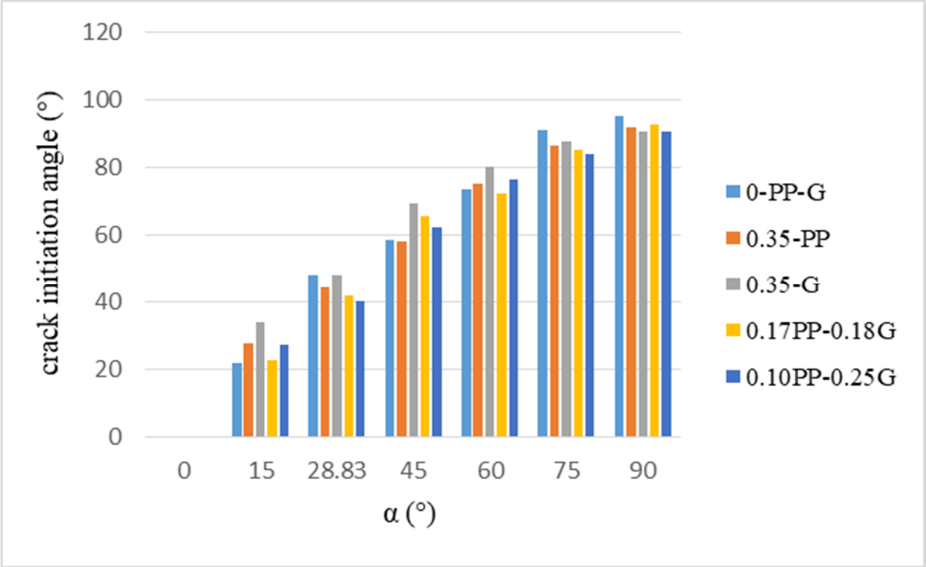

Figure 16. Bar diagram of crack initiation angle versus crack inclination angle for specimen lacking fibers, micro-silica, and limestone powder and that reinforced by different percentages of glass and PP fibers containing micro-silica and limestone powder.

As mentioned earlier, wing cracks begin to grow at a distance of d from the pre-crack tip at inclination angles of 60°, 75°, and 90°. Notably, for the concrete specimen containing 0.18% G and 0.17% PP hybrid fibers, this distance is very shorter than concrete lacking fibers, micro-silica, and limestone powder. The distance *d* decreases by 83.43%, 52.71%, and 30.60% at the inclination angles of 60°, 75°, and 90° for the concrete specimens containing 0.18% G and 0.17% PP hybrid fibers relative to the concrete lacking fibers, micro-silica, and limestone powder.

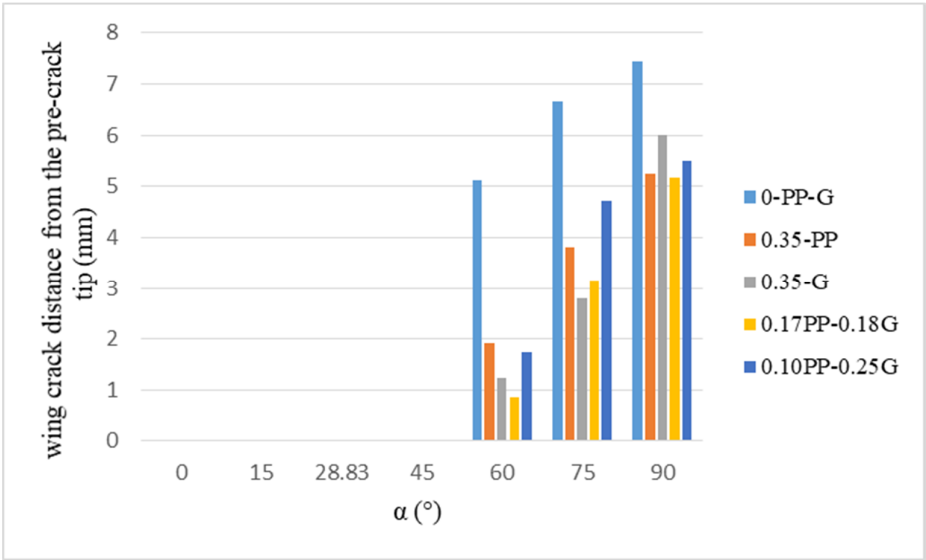

Figure 17. Bar diagram of wing crack distance from the pre-crack tip versus crack inclination angle for specimen lacking fibers, micro-silica, and limestone powder and that reinforced by different percentages of glass and PP fibers containing micro-silica and limestone powder.

As shown, the concrete specimens reinforced by 0.18% G and 0.17% PP hybrid fibers containing micro-silica and limestone powder has the highest effective fracture toughness relative to concrete lacking fibers, micro-silica, and limestone powder, concrete reinforced by 0.35% PP fibers containing micro-silica and limestone powder, concrete reinforced by 0.35% glass fibers

containing micro-silica and limestone powder, and concrete reinforced by 0.25% G and 0.1% PP hybrid fibers containing micro-silica and limestone powder. In loaded concrete specimens reinforced by 0.17% PP and 0.18% G hybrid fibers containing micro-silica and limestone powder and those reinforced by 0.1% PP and 0.25% G hybrid fibers containing micro-silica and limestone powder with a crack inclination angle of 15°, tensile cracks are initiated from two crack tips with an angle of 27° relative to the crack direction and reach the upper and lower boundaries. In loaded specimens with an inclination angle of 28.83°, wing cracks are initiated from two crack tips with an angle of 41° relative to the crack direction and reach the upper and lower boundaries. In loaded specimens with an inclination angle of 45°, wing cracks are initiated with an angle of 64° relative to the crack direction and reach the upper and lower boundaries. In loaded specimens with an inclination angle of 60°, wing cracks are initiated from two crack tips with an angle of 74° relative to the crack direction and reach the upper and lower boundaries. In loaded specimens with an inclination angle of 75°, wing cracks are initiated from the vicinity of two crack tips (not the pre-crack tips) with an angle of 86° relative to the crack direction and reach the upper and lower boundaries. In the specimens with a crack inclination angle of 90° (horizontal crack), a crack is first initiated at a distance of d from the crack tip in the lower semi-circle of the disc and then reaches the lower boundary with an angle of 90° relative to the pre-crack. Thereafter, another crack is initiated in the upper semi-circle at the same point, and reaches the upper boundary. Finally, two secondary cracks are exactly initiated from the main crack tip, and reaches the upper boundary.

5. Conclusion

The main results are summarized as follows:

- Using 10% micro-silica and 5% limestone powder improved the effective, mode I, and mode II fracture toughness of fiber-reinforced concrete specimens relative to concrete lacking fibers, micro-silica, and limestone powder. The concrete specimens reinforced by 0.17% PP and 0.18% G hybrid fibers containing micro-silica and limestone powder showed the highest effective fracture toughness and mode I and mode II fracture toughness. The effective and mode I fracture toughness increased by 6.38% and 8.14% at the inclination angles of 0° and 90° relative to the conventional concrete lacking micro-silica and limestone powder. The mode II fracture toughness occurring at 28.83° increased by 27.53% relative to the conventional concrete lacking micro-silica and limestone powder.
- The crack initiation angle of all specimens increased with increasing the crack inclination angle. The wing cracks were propagated in a curvilinear path to the disc edge parallel to the loading direction by continuing loading.
- The lowest load at failure was observed at a crack inclination angle of 45° for concrete lacking fibers, specimen reinforced by 0.35% PP fibers, and that reinforced by 0.1% PP and 0.25% G hybrid fibers. However, the lowest load at failure was observed at a crack inclination angle of 60° for the specimen reinforced by 0.17% PP and 0.18% G hybrid fibres.
- The cracks were initiated at inclination angles equal to and less than 45° with the growth of wing cracks from the pre-existing crack tip. However, the cracks were initiated at a distance of d from the pre-crack tip when the inclination angle increased and reached 60°, 75°, and 90°. The distance *d* decreases by 83.43%, 52.71%, and 30.60% at the inclination angles of 60°, 75°, and 90° for the concrete specimens containing 0.18% G and 0.17% PP hybrid fibers relative to the concrete lacking fibers, micro-silica, and limestone powder.
- The highest load at failure was observed for the concrete specimens containing micro-silica and limestone powder reinforced by 0.17% PP and 0.18% G hybrid fibers.

References

[1]. Haeri, H., Shahriar, K., Fatehi Maraji, M., and Maraefvand, P. (2013). The use of displacement discontinuity method in analyzing crack propagation mechanism in pseudo-rock materials, Analytical and Numerical Methods in Mining Engineering, Vol. 5, 38-49.

[2]. Payro, P. (2013). Fiber-reinforced concrete, Tehran, Farhand and Danesh.

[3]. Yazıcı, Ş., İnan, G. and Tabak, V. (2007). Effect of aspect ratio and volume fraction of steel fiber on the mechanical properties of SFRC. Construction and Building Materials. 21 (6): 1250-1253.

[4]. Song, P.S. and Hwang, S. (2004). Mechanical properties of high-strength steel fiber-reinforced concrete. Construction and Building Materials. 18 (9): 669-673.

[5]. Karahan, O. and Atiş, C.D. (2011). The durability properties of polypropylene fiber reinforced fly ash concrete. Materials & Design. 32 (2): 1044-1049.

[6]. Choi, Y. and Yuan, R.L. (2005). Experimental relationship between splitting tensile strength and compressive strength of GFRC and PFRC. Cement and Concrete Research. 35 (8): 1587-1591.

[7]. Prathipati, S.T. and Rao, C.B. K. (2020). A study on the uniaxial behavior of hybrid graded fiber reinforced concrete with glass and steel fibers. Materials Today: Proceedings, 32, 764-770.

[8]. AR, T.F. and Soheili, H. (2016). Combined effect of glass fiber and polypropylene fiber on mechanical properties of self-compacting concrete. Magazine of Civil Engineering, (2 (62)), 26-31.

[9]. Aslani, F. and Nejadi, S. (2013). Self-compacting concrete incorporating steel and polypropylene fibers: Compressive and tensile strengths, moduli of elasticity and rupture, compressive stress–strain curve, and energy dissipated under compression. Composites Part B: Engineering, 53, 121-133.

[10]. Patel, K., Gupta, R., Garg, M., Wang, B. and Dave, U. (2019). Development of FRC materials with recycled glass fibers recovered from industrial GFRP-acrylic waste. Advances in Materials Science and Engineering.

[11]. Jorbat, M.H., Hosseini, M. and Mahdikhani, M. (2020). Effect of polypropylene fibers on the mode I, mode II, and mixed-mode fracture toughness and crack propagation in fiber-reinforced concrete. Theoretical and Applied Fracture Mechanics, 109, 102723.

[12]. Ghazvinian, A., Nejati, H.R., Sarfarazi, V. and Hadei, M.R. (2013). Mixed mode crack propagation in low brittle rock-like materials. Arabian Journal of Geosciences. 6 (11): 4435-4444.

[13]. Golewski, G.L. and Gil, D.M. (2021). Studies of fracture toughness in concretes containing fly ash and silica fume in the first 28 days of curing. Materials. 14 (2): 319.

[14]. Abou El-Mal1, H.S.S., Sherbini, A.S. and Sallam, H.E.M. (2015). Mode II Fracture Toughness of Hybrid FRCs, International Journal of Concrete Structures and Materials Vol. 9, No. 4, pp. 475–486.

[15]. Akbardoost, J. and Ayatollahi, M.R. (2014). Experimental analysis of mixed mode crack propagation in brittle rocks: The effect of non-singular terms. Engineering Fracture Mechanics, 129, 77-89.

[16]. Iran Boress Co. Catalogue, 2019.

[17]. Institute of Standards and Industrial Research of Iran. (2015). Concrete aggregates-properties, Standard No. 302.

[18]. Institute of Standards and Industrial Research of Iran. (2013). Mixing room, moist chamber, moist room, and water ponds used in hydraulic testing of cement and concretes, Standard No. 17040.

[19]. Krishnan, G.R., Zhao, X.L., Zaman, M., and Roegiers, J.C. (1998). “Fracture Toughness of a Soft Sandstone”, Int. J. Rock Mech. Min. Sci. Vol. 35, No. 6, pp. 695-710.

[20]. Funatsu, T., Kuruppu, M. and Matsui, K. (2014). Effects of temperature and confining pressure on mixed-mode (I–II) and mode II fracture toughness of Kimachi sandstone. International Journal of Rock Mechanics and Mining Sciences, 67, 1-8.

[21]. Mirzaei Nasirabad, H., Jalali, S.M.E., Shariati, M., and Kakaei, R. (2010). Experimental study of crack growth in notched Brazilian plaster discs and effect of crack slope on failure behavior, Analytical and Numerical Methods in Mining Engineering, Vol. 1.

بررسی آزمایشگاهی اثر الیاف ترکیبی شیشه و پلی پروپیلن بر چقرمگی شکست حالت I، حالت II و حالت ترکیبی I-II بتن حاوی میکروسیلیس و پودر سنگ آهک

دانیال فخری، مهدی حسینی* و مهدی مهدی خانی

گروه مهندسی معدن، دانشگاه بین المللی امام خمینی (ره)، قزوین، ایران

ارسال ۲۰۲۲/۰۵/۲۰، پذیرش ۲۰۲۲/۰۵/۲۹

* نویسنده مسئول مکاتبات: mahdi_hosseini@eng.ikiu.ac.ir

چکیده:

چقرمگی شکست یکی از مهم‌ترین خواص بتن است که شرایط گسترش ترک و در نهایت شکست بتن را کنترل می‌کند؛ بتن، به‌عنوان پرکاربردترین مصالح در مهندسی عمران بوده که معمولاً ارزان‌ترین و رایج‌ترین مصالح موجود را در خود دارد. ازاین‌رو به سبب بروز ترک و شکستگی می‌تواند خسارت‌های جبران‌ناپذیری را به بار آورد. به این منظور در سال‌های اخیر با ساخت بتن‌های الیافی مسلح، تا حدود زیادی ضعف‌های مذکور در آن بهبود یافته است. در این مقاله با استفاده از روش آزمون روی دیسک برزیلی دارای ترک مستقیم (BD)، پیش‌بینی روند انتشار ترک و چقرمگی شکست در نمونه‌های مختلف بتنی بررسی شده است. این نمونه ها شامل بتن معمولی فاقد میکروسیلیس و پودرسنگ آهک و نمونه‌های با درصدهای حجمی مختلف الیاف شامل نمونه‌های بتنی دارای ۰/۳۵درصد الیاف تکی پلی‌پروپیلن، نمونه‌های بتنی دارای ۰/۳۵ درصد الیاف تکی شیشه، نمونه‌های بتنی دارای الیاف ترکیبی پلی پروپیلن و شیشه دارای۰/۱۷ درصد پلی‌پروپیلن و ۰/۱۸ درصد شیشه و نمونه‌های بتنی دارای الیاف ترکیبی پلی پروپیلن و شیشه دارای۰/۱ درصد پلی‌پروپیلن و ۰/۲۵ درصد شیشه می شود. در همه نمونه های بتن مسلح الیافی، میکروسیلیس جایگزین ۱۰ درصد وزن سیمان و پودرسنگ آهک جایگزین ۵ درصد وزن سیمان شده است. فرآیند گسترش ترک از شکاف‌های از پیش موجود در نمونه‌ها و همچنین چقرمگی شکست در حالت‌های I، II و حالت ترکیبی I-II محاسبه شد. آزمایش دیسک برزیلی بر روی نمونه‌های مورد مطالعه در زوایای انحراف ترک ۰، ۱۵، ۲۸/۸۳، ۴۵، ۶۰، ۷۵ و ۹۰ درجه انجام شده است. پس از مطالعات آزمایشگاهی مشخص گردید که شروع ترک‌های باله‌ای در زوایای کم‌تر از ۶۰ درجه ($0<\alpha<60$)، از نوک ترک از پیش موجود اتفاق می‌افتد و با ادامه‌ی بارگذاری مسیر رشد و انتشار ترک به راستای بارگذاری نزدیک می‌گردد. این در حالی است که برای زوایای ۶۰ درجه و بزرگ‌تر از آن، شروع ترک با فاصله d از نوک ترک آغاز می‌گردد. این فاصله در نمونه‌های فاقد الیاف بیشتر از نمونه‌های حاوی الیاف است. نمونه های دارای الیاف ترکیبی شامل ۰/۱۷ درصد الیاف پلی پروپیلن و ۰/۱۸ درصد الیاف شیشه و حاوی میکروسیلیس و پودر سنگ آهک بیشترین چقرمگی شکست مود I، II و ترکیبی I-II را نسبت به سایر نمونه های بتنی دارد.

کلمات کلیدی: چقرمگی شکست، میکروسیلیس، پودر سنگ آهک، الیاف ترکیبی شیشه و پلی پروپیلن، مود ترکیبی I-II .